Bifurcation to polarization self-modulation in vertical-cavity surface-emitting lasers

M. Sciamanna[1], T. Erneux[2], F. Rogister[1], O. Deparis[1], P. Mégret[1] and M. Blondel[1]

[1]Service d'Electromagnétisme et de Télécommunications
Faculté Polytechnique de Mons, 31 Boulevard Dolez, B-7000 Mons (Belgium)
[2]Optique Non-Linéaire Théorique
Université Libre de Bruxelles, Campus Plaine C.P. 231, B-1050 Bruxelles (Belgium)

We analyze the bifurcation mechanisms leading to polarization self-modulation (PSM) in a vertical-cavity surface-emitting laser (VCSEL) subject to a 90° polarization rotating external optical feedback. We show that the laser system undergoes a sequence of steady states and Hopf bifurcations to time-periodic solutions as we increase the feedback rate. Branches of PSM are obtained for moderate to high feedback rates and, using continuation methods, we show that they connect two orthogonally polarized external cavity modes (ECMs). This last result allows us to interpret PSM as a beating mechanism between ECMs and is in agreement with previous experiments.

Introduction

In general, the light emitted by a cylindrical VCSEL is linearly polarized (LP) along one of two preferential directions (called x and y) [1]. Polarization self-modulation (PSM) has been experimentally observed in a VCSEL subject to an optical feedback through a quarter-wave plate (QWP) whose optical axis is at 45° according to the VCSEL eigenaxes [2-6]. Every round-trip time, the quarter-wave plate rotates by 90° the polarization of the light reentering the laser cavity. The light is then observed to switch periodically between x- and y-linear polarizations with a period close to twice the external cavity round-trip time.

Previous numerical studies [4,5,7] have successfully reproduced the typical time traces observed experimentally. However, the origin of PSM has not yet been elucidated. In this paper, we show that PSM results from a Hopf bifurcation mechanism. Closed branches of time-periodic solutions corresponding to PSM connect two stable external-cavity modes (ECMs) and allow to interpret PSM as a beating mechanism between ECMs.

Modeling the laser system.

Our numerical simulations use two-mode rate equations [5,8] extended to optical feedback through a quarter-wave plate. In dimensionless form [9] they are given by

$$\frac{dE_x}{ds} = \frac{1}{2}(1+i\alpha)\left[(1+2Z)F_x - 1\right]E_x + \eta E_y(s-\theta)\exp(-i\phi_f), \tag{1}$$

$$\frac{dE_y}{ds} = \frac{1}{2}(1+i\alpha)\left[(1+2Z)F_y - 1\right]E_y + \eta E_x(s-\theta)\exp(-i\phi_f), \tag{2}$$

$$T\frac{dZ}{ds} = P - Z - (1+2Z)\left(F_x|E_x|^2 + F_y|E_y|^2\right), \tag{3}$$

where

$$F_x = 1-\varepsilon_{xx}\left(|E_x|^2 - \frac{P}{2}\right) - \varepsilon_{xy}\left(|E_y|^2 - \frac{P}{2}\right),\ F_y = 1-\varepsilon_{yx}\left(|E_x|^2 - \frac{P}{2}\right) - \varepsilon_{yy}\left(|E_y|^2 - \frac{P}{2}\right). \tag{4}$$

In these equations, E_x and E_y are the slowly varying linearly polarized components of the optical field and Z is the carrier density. s is time measured in units of the photon lifetime. α is the linewidth enhancement factor and $T \equiv \tau_s / \tau_p$ is the ratio of the carrier lifetime τ_s and photon lifetime τ_p. η is the feedback rate normalized by τ_p^{-1}. θ is the round-trip time in the external cavity $\tau \equiv 2L/c$ divided by τ_p, where L is the external cavity length and c is the speed of light. ϕ_f is the feedback phase. P is the pump parameter above threshold. Finally, F_x and F_y are two gain compression functions, where ε_{xx}, ε_{yy} represent the self-compression coefficients and ε_{xy}, ε_{yx} denote the cross-compression ones. Typical values for the parameters are given by: P = 0.4, T = 1000, α = 3, $\varepsilon_s = \varepsilon_{xx} = \varepsilon_{yy}$ = 0.02, and $\varepsilon_c = \varepsilon_{xy} = \varepsilon_{yx}$ = 0.04. The case of a short external cavity is considered (θ = 100). For simplicity, we consider ϕ_f = 0 and η is our control or bifurcation parameter.

Steady states and their stability

The steady state solutions of Eqs. (1)-(4) are solutions of the form

$$E_x = X \exp\left[i\left(\omega s + \phi_x\right)\right], E_y = Y \exp\left[i\left(\omega s + \phi_y\right)\right], \quad (5)$$

where the amplitudes X and Y and the phases ϕ_x, ϕ_y are constant. Introducing (5) into Eqs. (1)-(4) leads to five equations for X, Y, Z, $\Delta \equiv \phi_x - \phi_y$,ω, which can be analyzed analytically. We conclude that two sets of steady states can be distinguished depending on whether X=Y or X≠Y.

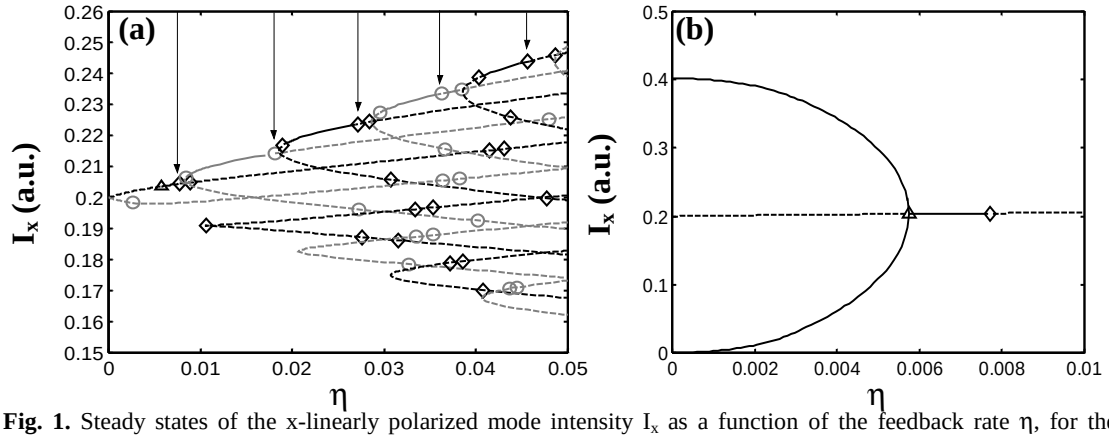

Fig. 1. Steady states of the x-linearly polarized mode intensity I_x as a function of the feedback rate η, for the parameters specified in the text. Figure 1 (a) represents the LK ECMs and antiLK ECMs in black and gray, respectively. Δ denotes a steady state bifurcation point to EPSS solutions shown in Fig. 1 (b), for clarity. o and ◊ correspond to antiLK and LK Hopf bifurcation points. Stable and unstable branches are shown by thick and dashed lines, respectively. The arrows indicate the bifurcation points from which emerge stable periodic branches.

Figure 1(a) shows the steady states corresponding to X=Y. The intensity $I_x \equiv X^2$ is plotted as a function of the feedback rate η and for the parameters listed above. This first set of steady states corresponds to two combs of external-cavity modes (ECMs), called LK and antiLK. They differ by the steady state value of Δ : Δ=0 for the LK ECMs while Δ=π for the antiLK ECMs. LK and antiLK ECMs correspond to LP light along the QWP eigenaxes. As shown in Fig. 1 (a), except for the first ECM, LK and antiLK ECMs appear in pairs through saddle-node bifurcation. The branch corresponding to the saddle (the ECM from the pair which has the lowest intensity) is always unstable and the corresponding ECM is called an antimode [10]. The branch corresponding to the

node can be stable. In our laser system, this ECM is not stable directly when it is created from the saddle-node bifurcation but becomes stable through a Hopf bifurcation point at a feedback rate slightly larger. A stable ECM is called a mode. The LK or antiLK modes become unstable through a Hopf bifurcation point.

Figure 1(b) shows the steady states corresponding to X≠Y. Two branches of steady states are possible: I_x can follow the upper (lower) branch of steady states and I_y follows respectively the lower (upper) branch. The two branches become unstable through a pitchfork bifurcation with the first LK ECM. We can show that these steady states only appear for the condition $\varepsilon_c > \varepsilon_s$ and they remain confined to low feedback rates. Since Δ is in general different from π, they correspond to elliptically polarized steady states (EPSS).

Route to PSM

Figure 2 shows the bifurcation diagram of I_x as a function of the feedback rate. This illustrates the route to PSM in the laser system. Accordingly to the experiment, the VCSEL emits in only one mode (x or y) at zero feedback, and as soon as the feedback rate increases EPSS appear.

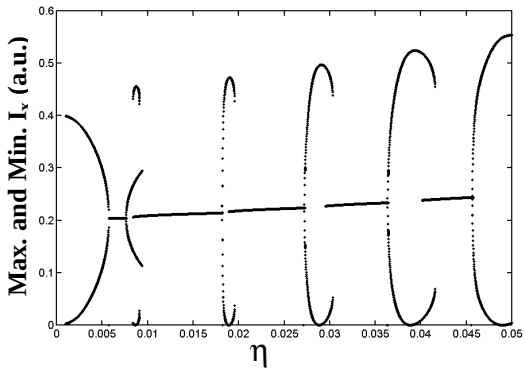

Fig. 2. Bifurcation diagram for I_x as a function of the feedback rate η, for the parameters quoted in the text.

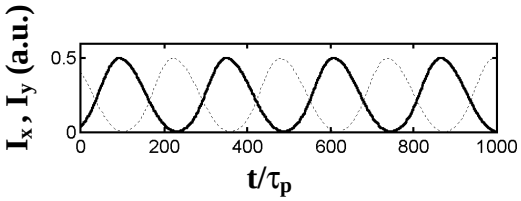

Fig. 3. I_x, I_y, as a function of time, for η = 0.04. This figure illustrates PSM.

EPSS loose stability through a pitchfork bifurcation. For larger feedback rates, the laser system evolves into a sequence of LK and antiLK ECMs and Hopf bifurcation to time-periodic solutions. Figure 3 shows the time-periodic solutions corresponding to one of the branch emerging from a Hopf bifurcation point on ECM. X and Y-LP modes evolve periodically in antiphase, with a period close to 2θ. This corresponds to the experimentally observed PSM. We observe also from Fig. 2 that high feedback rate stabilize the PSM.

Bifurcation bridges between ECMs lead to PSM

We gain physical insight into PSM by continuing [11] the unstable parts of the branches of time-periodic solutions shown in Fig. 2. In Fig. 2 branches of PSM overlap two ECMs with a small bistable region. This suggests that PSM is created by the interaction between two consecutive ECMs. Figure 4 shows indeed that the branch emerging from a Hopf bifurcation point on antiLK mode becomes unstable through a limit point on cycle and connects to a stable Hopf point on a LK mode.

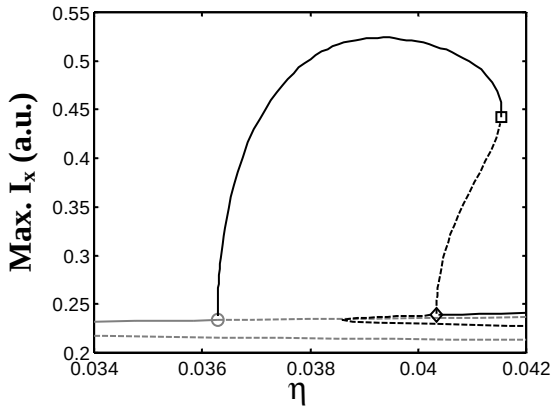

Fig. 4. Bifurcation bridge between ECMs. The maximum of I_x is represented as a function of η. The same symbols as in Fig. 1 mark the Hopf bifurcation points. □ denote limit points of periodic solutions.

Closed branches of time-periodic solutions connect antiLK and LK modes and allow us to interpret PSM as a beating mechanism between ECMs. The PSM frequency is therefore related to the difference between the two ECM frequencies and in general depends on the feedback rate. We have observed such a dependency numerically and our physical intepretation is in good agreement with experimental results [2-6]. Our results show also that a connection between two modes through a branch of periodic solution is possible in a delayed semiconductor laser system. This result has not been documented before and substantiates recent reports of bridges between mode and antimode through time-periodic solutions [12].

Conclusions

We have shown that the experimentally observed PSM in VCSELs comes from a Hopf bifurcation mechanism on ECMs. A route to PSM was shown involving more complex dynamical behaviors than just PSM. This motivates new experimental investigations on the bifurcation diagram. Furthermore, physical insight into PSM has been given by showing that PSM results from a beating between two modes. Bifurcation bridges between modes are shown here for the first time and motivate new studies on delayed laser systems.

The authors acknowledge support from the FNRS (Belgium) and the IAP IV-07 project of the Belgian government. The research of TE is also supported by the U.S. Air Force Office of Scientific Research Grant No. AFOSR F49620-98-1-0400 and the National Science Foundation Grant No. DMS-9973203.

References

[1] A.K. Jansen van Doorn, M.P. Van Exter, and J.P. Woerdman, Appl. Phys. Lett. **69**, 1041 (1996).

[2] S. Jiang, Z. Pan, M. Dagenais, R.A. Morgan and K. Kojima, Appl. Phys. Lett. **63**, 3545 (1993).

[3] N. Badr, I.H. White, M.R.T. Tan, Y.M. Young, and S.Y. Wang, Electron. Lett. **30**, 1227 (1994).

[4] F. Robert, P. Besnard, M.L. Chares, and G.M. Stephan, IEEE J. Quantum Electron. **QE-33**, 2231 (1997).

[5] H. Li, A. Hohl, A. Gavrielides, H. Hou, and K.D. Choquette, Appl. Phys. Lett. **72**, 2355 (1998).

[6] G. Ropars, P. Langot, M. Brunel, M. Vallet, F. Bretenaker, A. Le Floch, and K.D. Choquette, Appl. Phys. Lett. **70**, 2661 (1997).

[7] C. Masoller, and N.B. Abraham, Appl. Phys. Lett. **74**, 1078 (1999).

[8] Y.C. Chen and J.M. Liu, Appl. Phys. Lett. **50**, 1406 (1987).

[9] P.M. Alsing, V. Kovanis, A. Gavrielides, and T. Erneux, Phys. Rev. A **53**, 4429 (1996).

[10] J. Mork, B. Tromborg, and J. Mark, IEEE J. Quantum Electron. **QE-28**, 93 (1992).

[11] K. Engelborghs,''DDE-BIFTOOL: a Matlab package for bifurcation analysis of delay differential equations'', http://www.cs.kuleuven.ac.be/koen/delay/ddebiftool.shtml.

[12] D. Pieroux, T. Erneux, B. Haegeman, K. Engelborghs, D. Roose, to be published in Phys. Rev. Lett.